Analyst

Visualizing Mass Transport in Desorption Electrospray Ionization using Time-of-Flight Secondary Ion Mass Spectrometry: A Look at the Geometrical Configuration of the Spray

Journal:	*Analyst*
Manuscript ID:	AN-ART-08-2014-001481.R1
Article Type:	Paper
Date Submitted by the Author:	03-Sep-2014
Complete List of Authors:	Muramoto, Shin; National Institute of Standards and Technology, Materials Measurement Science

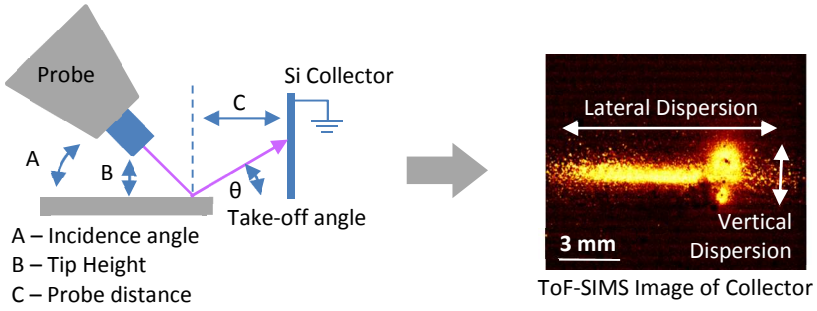

The desorption profile of analyte molecules desorbed by desorption electrospray ionization was imaged and characterized using time-of-flight secondary ion mass spectrometry

Visualizing Mass Transport in Desorption Electrospray Ionization using Time-of-Flight Secondary Ion Mass Spectrometry: A Look at the Geometric Configuration of the Spray

Shin Muramoto

National Institute of Standards and Technology, Gaithersburg, MD 20899, USA
1-301-975-5997 (phone)
1-301-417-1321 (fax)
shinichiro.muramoto@nist.gov

Abstract

Time-of-flight secondary ion mass spectrometry (ToF-SIMS) was used to visualize the transport of analyte molecules desorbed onto a silicon wafer collection substrate by desorption electrospray ionization (DESI). The effect of spray incidence angle, tip height, and probe distance on the concentration and the spatial distribution of desorbed analyte molecules, was investigated with the objective of identifying DESI operational parameters that provide more reproducible results by achieving steady ion transmission and minimized material loss. An incidence angle between 25° and 35° with respect to the plane of the surface provided the best compromise between maximizing ambient MS signal and achieving the best reliability. Glancing incidence angles provided higher ambient MS signals through a tighter dispersion of the secondary droplet plume, but run-to-run variability of as much as 40%. On the other hand, steeper incidence angles led to a widening of the lateral dispersion of the secondary droplets and decreased analyte desorption. For all incidence angles, shorter probe distances were preferred since the resulting tighter dispersion of the secondary droplets produced higher ion transmission and therefore higher ambient MS signals. Tip height was found to correlate with the spot size (footprint) of the spray on the surface; changing the tip height from (1 to 2 to 3) mm changed the diameter of the spray impact area from (1.3, 1.8, to 2.1) mm, respectively. For shorter probe to MS inlet distances, larger tip heights increased the ambient MS signal due to increased analyte desorption while maintaining a tighter dispersion of the secondary droplet plume. Equally important to optimizing instrument configuration was the understanding that the deposition of a sample onto the surface resulted in a coffee ring, where the diameter was larger than the spot size of the spray. Higher tip heights may be preferred for a more consistent analyte response since all or a large fraction of the analyte could be sampled to reduce variability in ambient MS response. The study showed that ToF-SIMS can be used as a unique tool for characterizing the transport of desorbed analyte molecules for DESI, and potentially offering insight into new interface designs for improved transmission of analyte into the mass spectrometer.

Keywords: ambient ionization, desorption electrospray ionization, tof-sims

Introduction

Desorption electrospray ionization (DESI) uses pneumatically-assisted nebulization to emit charged solvent-droplets that impinge a surface to generate analyte-laden secondary droplets.[1-5] The charged primary droplets impinge the sample surface, solvate the analyte into a thin liquid film, and expel analyte-laden secondary droplets through the transfer of momentum from the impingement of successive high velocity primary droplets.[1, 4] The secondary droplets then enter the mass spectrometer (MS) inlet and experience droplet evaporation and ionization effects similar to conventional electrospray ionization through a charge residue mechanism or ion evaporation.[6-7] With the development of DESI for ambient surface mass spectrometry,[8-9] it has found numerous areas of application including biological tissue analysis,[10-13] pharmaceutics,[14-16] forensics,[17-20] and explosives.[1-2, 18, 21] In addition, its development has sparked a rapid increase in the number of new ionization and desorption methods that operate in atmosphere.[22]

One major attribute that contributed to the expansion of DESI and other ambient ionization techniques was the ability to directly analyze samples in their native environment with minimal sample preparation, in comparison to more traditional surface chemical analytical techniques such as secondary ion mass spectrometry (SIMS) and x-ray photoelectron spectroscopy (XPS) that require analysis to take place inside a vacuum. Other attributes such as low cost, portability, and high-throughput have undoubtedly helped expand ambient techniques to a wide range of application areas. However, the technique's sample-to-sample repeatability is associated with a large degree of uncertainty, highlighted by literature indicating the need to configure instrument geometry, type of analyte, substrate, spray solution chemistry, and even the type of mass analyzer in order to obtain repeatable measurements.[8, 23-26] This has been further emphasized by a recent interlaboratory study of repeatability in DESI sponsored by VAMAS (Versailles Project in Advanced Materials and Standards).[27] The careful characterization of ion transport behavior is therefore critical for advancing the use of the technique.

A number of studies have investigated and characterized the fundamental aspects of droplet dynamics and ionization mechanisms, including charge transmission,[28-29] spray plume and spot size,[30-32] primary and secondary droplet dynamics,[5] and computational fluid dynamics (CFD) simulations of secondary droplet formation.[33-34] However, the knowledge of the transport of desorbed analyte molecules into the MS interface, with respect to how it can improve the

reproducibility of the technique, is still relatively limited. In this manuscript, time-of-flight secondary ion mass spectrometry (ToF-SIMS) was used to elucidate this process by directly imaging the spatial distribution of analyte molecules desorbed by DESI. The effect of probe incidence angle, height, and distance on the relative amount and the spatial distribution of desorbed analyte molecules captured on collector surfaces were investigated, with the objective of qualitatively identifying settings that would maximize signal, minimize material loss, and produce consistent results. The ultimate goal is to use ToF-SIMS to provide visual desorption profile data that can be used to improve ambient MS interface designs for optimal collection of analyte molecules.

Experiment

Sample Preparation. Cocaine hydrochloride dissolved in methanol at a concentration of 1 mg/mL was purchased from Restek* (Bellefonte, PA) and further diluted down to 100 µg/mL in methanol (Sigma-Aldrich Co., St. Louis, MO). Aliquots of 2 µL each of the diluted cocaine solution were deposited onto 3 mm diameter polytetrafluoroethylene (PTFE, or Teflon®) hydrophobic wells of a standard Prosolia Omni Slide (Indianapolis, IN), and allowed to air dry prior to analysis. 10 cm Si(100) wafers purchased from Virginia Semiconductors (Fredericksburg, VA) were diced into 15 mm × 15 mm square pieces using the Disco DAD341 dicing saw equipped with a metal blade (Tokyo, Japan). The individual pieces were soaked overnight in an 18 MΩ/cm deionized water obtained from a Milli-Q ultrapure water system (EMD Millipore, Billerica MA) to remove salts, and sonicated for 15 min each in acetone and methanol to remove organic contaminants.

Contact angle measurements on the Omni Slides were made using an FTA125 contact angle goniometer (First Ten Angstroms, Portsmouth, VA) with ultrapure water and methanol/water solution as the liquid phase. The drop volume was 2 µL, and the contact angles were calculated using the FTA software assuming a symmetrical droplet.

Ambient Pressure Ionization Source. The droplet-based DESI source consisted of a Prosolia Omni Spray® ion source with a solution composition and instrument configuration described in detail elsewhere.[35] Briefly, a 1:1 methanol/water solution (Chromasolv® Sigma Aldrich, St. Louis, MO) in a 1 mL gastight syringe was delivered at a flow rate of 3 µL/min using a Legato 100 syringe pump from KD Scientific (Holliston, MA). The spray was directed

toward the surface using a charging potential of +4000 V at various incidence angles with respect to the sample. Droplet nebulization was pneumatically-assisted with a N_2 coaxial carrier gas supplied at (552 ± 14) kPa (80 psig). The impact of carrier gas pressure was not investigated at this time. Mass analysis was performed using the Applied Biosystems/MDS Sciex 4000 QTrap mass spectrometer (Framingham, MA), with the following instrument parameters: curtain gas pressure of 138 kPa (20.0 psi), ion source gas pressure of 83 kPa (12.0 psi), interface heater temperature of 150 °C; declustering potential of +130 V; and an entrance potential of +10 V. A stainless steel inlet capillary with a length of 30 mm, outer diameter of 3 mm, and inner diameter of 1.5 mm was attached to the atmosphere-vacuum interface of the QTrap. 2 µL aliquots of 100 µg/mL solution of cocaine were deposited on each PTFE deposition area, for a total deposit of 200 ng of analyte per spot. Each area was exposed to the DESI spray for 180 s while the data was acquired. For collection experiments, each spot containing the analyte was exposed for 10 s. The exposure time was controlled using a manual shutter described in Figure 1.

Time-of-Flight Secondary Ion Mass Spectrometry. The collection substrates were imaged using an IONTOF IV (Münster, Germany) ToF-SIMS instrument equipped with a 25 kV Bi_3^+ analysis source oriented at an incident angle of 45º. The analysis beam at a current of 0.12 pA pulsed current, operated at a frequency of 10 kHz, was rastered within a 500 µm × 500 µm area with a pixel density of 128 pixels/mm. 5 scans were summed at each position for an ion dose of 2.45×10^9 ions/cm^2, which is far below the static limit of 1×10^{12} ions/cm^2. These scans were stitched together to create a 14 mm × 10 mm image, which were then cropped to obtain the images presented in the figures. The dimensions of the desorption profile were calculated from an average of three line scans across the deposition pattern, using 50 % of the maximum intensity to demarcate the edges.

*Certain commercial equipment, instruments, or materials are identified in this paper to adequately specify the experimental procedure. Such identification does not imply recommendation or endorsement by the National Institute of Standards and Technology, nor does it imply that the materials or equipment identified are necessarily the best available for the purpose.

Results and Discussion

The scope of this study was limited to investigating the effect of geometric configuration of the instrument on the desorption profile of the secondary droplets (spatial distribution of the desorbed analyte on the collectors). As shown in Figure 1a, the probe incidence angle, tip height, and probe distance were adjusted, and the analyte in the secondary droplets were either detected using the QTrap system (ambient MS) or were collected onto silicon wafers for visualization of the desorption profile using ToF-SIMS. The experiment used a module for holding the collection substrate that was built in-house, with the setup shown in Figure 1b. A sliding glass shutter in front prevented any overexposure of the DESI spray. The collector substrate was grounded to prevent any charge-buildup on the collector substrate. After the analytes were collected, the silicon wafer was imaged using ToF-SIMS to produce the ion image shown in Figure 1c.

The benefit of using ToF-SIMS for imaging was its ability to detect monolayer coverage of analyte on the surface. Imaging the surface of the collector after a very short exposure to the secondary droplet plume was similar to taking a "snapshot" photograph to visualize the instantaneous accumulation of analyte. Other imaging techniques that used fluorescent dyes and tracers would have required the accumulation of a relatively large amount of both analyte and tracers for imaging, both of which may diffuse out with longer exposure times and create an overestimated footprint on the particle collector.

For the collection experiment, the DESI spray was emitted without any applied potential. This was done for safety considerations, since the desorption profiles of the analytes on the surface with (+4000 kV) and without emitter voltages were indistinguishable (Figure S-1, Supplemental Information), showing that, for the conditions tested, the electric field in ambient conditions was negligible in influencing the trajectories of the secondary droplets. The analyte used was cocaine hydrochloride, a preformed ion that displays a very high ionization yield under ToF-SIMS analysis,[36] which was an ideal tracer for visualizing the spread of the secondary droplets. Moreover, picoammeter measurements of the DESI spray containing cocaine showed that no current was being measured when the emitter voltage was turned off (Figure S-2, Supplemental Information), which showed that charge buildup on the collector surface due to deposition of droplets was also negligible.

The effect of incidence angle on desorption profile and ambient MS response.

Relative to the plane of the surface, incidence angles of 20° to 75° in 5° intervals were used to give a more complete picture of how the desorption profile changed with incidence angle. ToF-SIMS images in Figure 2a showed that the desorption profiles for all incidence angles had a wide distribution of secondary droplets in the lateral direction due to the diverging flow of the spray jet, consistent with fluid dynamics simulations.[34] Interestingly, steeper incidence angles were associated with much wider lateral dispersions and thinner vertical dispersions, in addition to decreased material transfer, as evidenced by the reduced surface coverage of the analyte on the collectors. Above an incidence angle of 45°, the desorption profiles became increasingly fragmented, or less-contiguous in the sense that the collector surfaces became populated by larger droplets that were more widely spread across the collection surface. This was in contrast to glancing incidence angles below 45° where the desorption profiles appeared much more diffuse, with the secondary droplets much finer and in closer proximity to neighboring droplets.

In addition to the production of larger droplets, the desorption profiles obtained from steeper incidence angles were very inconsistent. The surface coverage of the analytes and their exact positions on the collectors were highly variable and could not be repeated. An example of this can be seen in the ion images of the collectors at incidence angles of 60°, 65°, 70° and 75°, where the overall distributions appeared similar but the secondary droplets were clearly not landing at the same location. Since the diameter of the ambient MS inlet orifice was rather small (1 mm ID, seen as the blue dot in Figure 1a), variations in the spatial distribution of the larger droplets were expected to significantly affect both the intensity and reproducibility of the ambient MS signal.

The ToF-SIMS intensity of cocaine normalized to the intensity of silicon (*m/z* 304 to *m/z* 28, to compensate for primary ion current variability since the acquisition time for each image was roughly 30 min) was plotted as a function of incidence angle, and presented in Figure 2b. As was expected, steeper incidence angles were associated with decreased normalized cocaine intensity. In the plot, the ToF-SIMS normalized intensity correlated roughly with the cosine of the incidence angle for angles between 25° and 65°. This suggested that for these incidence angles, the forward-component of the spray jet was primarily responsible for the amount of analyte being desorbed by the spray and collected onto the silicon wafer. This was suggested in computational fluid dynamics simulations,[33-34] where the dominant force responsible for

secondary droplet ejection is the transfer of momentum from the spray to the droplet pool on the surface. Not taking into account the surface or electrostatic effects on droplet ejection, a more glancing incidence angle with a larger forward momentum would simply be expected to expel a higher amount of analyte from the surface. Conversely, steeper incidence angles would be expected to expel less, and contribute more to the pool of solvent on the surface. This excess solvent, combined with lower forward momentum of the spray jet, may be the reason for the presence of larger diameter droplets on the collectors for incidence angles above 45°.

In comparison to the ToF-SIMS intensity versus incidence angle plot, the cocaine signal observed by the QTrap system (ambient MS) presented in Figure 2c showed a much faster decay in intensity. For example, the intensity decreased an order of magnitude when the incident angle was changed from 20° to 45°, while the ToF-SIMS normalized intensity decreased by a factor of two over the same interval. This rapid decay in intensity was most likely due to two factors. One, the widening of the lateral dispersion meant that less material was entering the MS through the small inlet orifice. Since the inlet orifice had an internal diameter of just 1 mm, any dispersion of the analyte-laden droplets would have led to a significant material loss (the size of the inlet orifice relative to the desorption profile can be seen in Figure 2a, inside the ion image acquired for an incidence angel of 20°). And two, larger diameter droplets generated by steeper incidence angles may not have had enough time to desolvate inside the MS inlet capillary. Even with heat applied to the inlet capillary, entry of droplets into the capillary does not automatically guarantee ionization because a large fraction of the spray will still consist of droplets and ion clusters formed during the collisional cooling and free expansion of gas inside the low-pressure region of the mass spectrometer.[37] Although the rate of desolvation can depend largely on instrumental configurations (such as heating temperature and nebulizing gas pressure), for the conditions tested, it seemed that the use of steeper incidence angles led to a relatively lower extent of desolvation due to the size of the droplets seen on the collector surfaces. To add to the complexity, the ABSciex instrument used in this study exhausted gas from the inlet to the atmosphere. Called the Curtain Gas™, dry nitrogen was pushed out of the inlet to drive neutral species and droplets away from the MS orifice to reduce contamination and sample crossover.[38-39]

Charged ions penetrate the curtain because they are electrostatically attracted toward the orifice by an electric field gradient. The Curtain Gas would be expected to further reduce the entry of material for steeper incidence angles.

Despite the presence of the Curtain Gas, the collection experiment is applicable for desorption analysis since numerous different types of MS instruments exist that are interfaced to DESI; some may have a setup similar to a Curtain Gas, while some may have negative pressure where even neutral secondary droplets may become entrained into the tube. This collection experiment provides a fundamental background of the droplet dynamics which the user can use to determine the best configuration for his instrument.

From the data presented, the use of glancing incidence angles was preferred due to greater analyte desorption, smaller transmission loss, and the formation of smaller secondary droplets. However, these conditions were associated with a large degree of run-to-run variability; as much as 40 % variability was observed for an incidence angle of 20° (see Table S-1 for a table of intensities, Supplemental Information). For steeper incidence angles, such as 55°, the variability was roughly 10%, which agreed well with the literature value of roughly 9% for a solution concentration of 100 μg/mL.[40] The reason for the large variability for glancing incidence angles is most likely due to the entry of excessive material into the MS inlet, which may have caused: an inefficient desolvation of the droplets; a saturation of the analyte concentration where too many molecules were competing for charge; and/or significant material loss from the secondary droplets wetting the inside wall of the inlet capillary and not reaching the vacuum interface. The analyte molecules trapped in the liquid film along the inside wall of the capillary could also have contributed to the variability from sample crossover. Due to these reasons, the most repeatable incidence angle was determined to be in the range between 25° to 35°. Despite a drop in ambient MS signal intensity, the tighter lateral dispersion of the secondary droplets suggested limited transmission loss, and a much smaller run to run variability implied a more efficient desolvation of the droplets.

The effect of tip height and probe distance on desorption profile. In addition to incidence angle, tip height and probe distance were also investigated. ToF-SIMS images in Figure 3 showed the desorption profiles collected at (3, 5, 7, 9, and 11) mm from the spray impact point at incidence angles of 30°, 45°, 60°, and 75°. This was performed at tip heights of 1

mm, 2 mm, and 3 mm. Looking collectively at the group of images in Figure 3, the general trend was increased mass transport for glancing incidence angles. As was discussed before, the use of glancing incidence angles were better at desorbing more analyte from the sample surface relative to steeper incidence angles, consistent with ToF-SIMS intensity results in Figure 2b. This relationship generally held true regardless of tip height and probe distance; at a given tip height and probe distance, increasing the incidence angle consistently led to decreased mass transfer. This was also seen to be true for tip height, where for a given incidence angle, increasing the tip height seemed to enhance mass transport.

In comparison, changing the probe distance while keeping incidence angle consistent gave mixed results; for incidence angles of 30° and 45°, desorption seemed to increase with distance, whereas for incidence angles of 60° and 75°, desorption seemed to decrease. Regardless, the investigation of longer probe distances seemed to reveal a secondary aspect of the desorption process, where there seemed to be a scattering of the droplets, marked by the increased presence of diffuse droplets on the outer fringes of the desorption profile. For an incidence angle of 75° and a probe distance of 9 mm and 11 mm, the extent of scattering was so high that almost no analyte was seen on the collectors. Scattering seemed to be caused by the collision of secondary droplets with gas molecules in atmosphere, since the extent of scattering increased consistently for longer probe distances. Impactor effects could have played a role in the scattering of droplets near the collector surface, [41-43] but a previous report comparing the desorption profiles on porous and non-porous substrates ruled this out.[44]

For incidence angles of 30° and 45°, changing the tip height and probe distance had significantly affected both the vertical and lateral dispersions of the desorption profile. In general, dispersions in both directions were seen to expand roughly linearly with probe distance, as plotted in Figure 4. For example, at an incidence angle of 30° and a tip height of 2 mm, the lateral dispersion expanded from (5.4, 7.7, 9.0, 10.0, to 11.3) mm, and the vertical dispersion expanded from (2.0, 2.5, 3.0, 3.5, to 4.3) mm for probe distances of (3, 5, 7, 9, and 11) mm, respectively (see Tables S-2 and S-3 for dimensions of all profiles, Supplemental Information). This linear trend was conserved for tip heights of 2 mm and 3 mm for both incidence angles of 30° and 45°. The expansion of the lateral dispersion with distance was expected since the secondary droplets were expelled at a particular dispersion angle as soon as the droplets left the spray impact area,[34] most likely due to the diverging flow of the DESI spray. The same reasoning

applied for the vertical dispersions at tip heights of 2 mm and 3 mm, however, at a tip height of 1 mm, the vertical dispersion was seen to stay constant or even slightly contract.

For incidence angles of 60° and 75°, changing the tip height and probe distance had significantly different effects on the lateral dispersion. In general, extensive scattering of the secondary droplets caused the lateral dispersions to visually contract rather than expand with distance, with the contraction occurring at a particular probe distance depending on the incidence angle. For example, at an incidence angle of 60° and a tip height of 2 mm, the lateral dispersion expanded initially, but began to taper beyond a probe distance of 7 mm; the lateral dispersions had changed from (7.3, 9.5, 9.9, 9.5, to 2.3) mm for probe distances of (3, 5, 7, 9, and 11) mm, respectively. As can be seen in Figure 4c, the same trend was seen for a tip height of 3 mm. In comparison, at an incidence angle of 75° and a tip height of 2 mm, the lateral dispersion decayed linearly, from (10.0, 7.0, 5.1, to 0) mm for probe distances of (3, 5, 7, and 9) mm, respectively, indicating significantly increased scattering of the secondary droplets.

It seemed that scattering can be limited if either the probe distance decreased or incidence angle became less steep. For the conditions tested (*i.e.,* 80 psig nebulizing gas, 3 µL/min solvent flow rate, probe height between 1 mm and 3 mm, 200 ng of analyte, exposure time of 10 s, the use of an Omni Slide surface, etc.), the data showed that scattering in the lateral direction can be limited if the combination of incidence angle and probe distance satisfied the following condition:

$$\cos\theta/d \; > 0.07 \qquad \text{(equation 1)}$$

where d is the probe distance in mm and θ is the incidence angle in degrees with respect to the sample surface. Not enough data were available to determine the effect of tip height on scattering. For an incidence angle of 60°, the values obtained using this relation were (0.17, 0.10, 0.071, 0.056, and 0.045) mm^{-1} for probe distances of (3, 5, 7, 9, and 11) mm, respectively. The values predicted a tapering of the lateral dispersion length at a probe distance of 7 mm for all tip heights, as seen in Figure 4c. This was also consistent with the increase in diffuse appearance of the desorption profiles in Figure 3c. For an incidence angle of 75°, the values obtained using Equation 1 were (0.086, 0.052, 0.037, 0.029, and 0.024) mm^{-1} for probe distances of (3, 5, 7, 9, and 11) mm, respectively. As can be seen in Figure 4d, the result was an immediate decay in the

dispersion length with probe distance, consistent with the gradual loss in intensity of the profiles in Figure 3d.

The equation was also applicable for glancing incidence angles. For an incidence angle of 45°, the values were (0.24, 0.14, 0.10, 0.079, and 0.064) mm^{-1} for probe distances of (3, 5, 7, 9, and 11) mm, respectively, indicating the onset of scattering at a distance of 11 mm. This was supported by the trend in Figure 4b for all tip heights, although this was hard to see in the profile images in Figure 3b. In comparison, an incidence angle of 30° did not show any decrease in lateral dispersion for the probe distances investigated. Equation 1 generated values of (0.29, 0.17, 0.12, 0.096, and 0.079) mm^{-1} at probe distances of (3, 5, 7, 9, and 11) mm, respectively. However, a theoretical probe distance of 13 mm gave a value of 0.067, suggesting that the tapering of the lateral dispersion could occur around this distance. These observations suggested that scattering of the secondary droplets in air can occur for all incidence angles, but will occur to a higher degree for steeper incidence angles.

Despite the divergent flow of the spray and the increase in lateral dispersion of the secondary droplets with probe distance (Figure 4), the angle of the dispersion was found to actually decrease with probe distance. As shown in Figure 5, the dispersion angle decayed linearly with probe distance for all incidence angles. In the lateral direction, the slopes of the trends were (-4.3 ± 0.8, -4.0 ± 1.0, -10.1 ± 2.1, and -14.7 ± 0.9) °/mm for incidence angles of 30°, 45°, 60°, and 75°, respectively, showing that the extent of scattering for the droplets traveling in the lateral direction was much higher for steeper incidence angles. It was not clear whether the higher scatter rate was caused by a slower droplet velocity or whether the larger-sized droplets were more likely to scatter due to an increased likelihood of collision with gas molecules. Regardless, the presence of scattering and the results of the dispersion angle indicated that material was being lost linearly with probe distance because the scattered droplets were unable to reach the collector surface. In comparison, the vertical dispersion angles shared a similar trend, but were not as heavily affected (Figure 5, open markers). In the vertical direction, the slopes varied from (-2.1 ± 1.0, -1.1 ± 0.2, -1.5 ± 0.3, and -1.7 ± 0.6) °/mm for incidence angles of 30°, 45°, 60°, and 75°, respectively. Scattering occurred to a similar extent, and was not found to be dependent on incidence angle. No convincing relationship was found between tip height and the extent of scattering.

From the results presented, it seemed that the distance between the spray impact point and the inlet of the MS was best kept minimal to avoid loss in ion transmission due to the divergent secondary droplet plume. By keeping the probe distance shorter, it ensured that a larger fraction of desorbed material would enter the MS inlet. Particularly at a probe distance of 3 mm, it seemed that the tip height had minimal effect on mass transfer since changing the tip height did not affect the shape of the desorption profile, but whether this is true or not will be discussed in the following section.

The effect of tip height and probe distance on ambient MS response. ToF-SIMS imaging was able to elucidate, to a certain degree, the effect of geometric configuration on the hydrodynamic properties of the DESI spray. The results presented in the previous sections showed how the density of the secondary droplet plume can be affected by probe distance: shorter probe distances were seen to produce tightly dispersed secondary droplet plumes, whereas longer probe distance were seen to result in wider dispersions and scattering. To find out whether these observations would correlate with the ambient MS intensities, the same experiments performed above were repeated using the ambient MS. The collection substrate was now replaced with the 30 mm long inlet capillary, and the probe distance became the distance between the spray impact point and the edge of the inlet capillary.

The plot of ambient MS intensity as a function of incidence angle, probe distance, and tip height are shown in Figure 6. As can be seen, the ambient MS signal showed a decrease in intensity as a function of probe distance for all incidence angles. In all cases, higher signals were seen for shorter probe distances, as a result of the tighter dispersion of the secondary droplet plume and increased ion transmission into the MS inlet. Interestingly, higher intensities were seen when the tip height was increased from (1 to 2 to 3) mm, with the largest changes seen at the shortest probe distance of 3 mm. Based on the images of the desorption profiles in Figure 3, one would have assumed that at a probe distance of 3 mm, the intensities would have been the same regardless of tip height since the area of the desorption profiles did not change. For example, at an incidence angle of 30° and a probe distance of 3 mm, the area of the desorption profiles at tip heights of (1, 2, and 3) mm were roughly the same (Figure 3a), but resulted in observed intensities of $(5.3 \pm 1.8) \times 10^6$ counts, $(9.5 \pm 0.5) \times 10^6$ counts, and $(1.4 \pm 0.2) \times 10^7$ counts, respectively, corresponding to a factor of 1.8 increase for a change in tip height from 1

mm to 2 mm, and a factor of 2.6 increase for a change in tip height from 1 mm to 3 mm. This suggested that the number of analyte molecules in the secondary droplet plume had increased due to an increased number of analyte molecules being desorbed from the surface.

Another item of discussion earlier was the perceived benefit of using longer probe distances, where the increased frequency of collision of the secondary droplets with atmospheric gas molecules would have accelerated the desolvation process, leading to an increased number of 'dry' ions that were available for detection. Unfortunately, the lower intensities at longer probe distances shown in Figure 6 indicated that no signal enhancement from accelerated desolvation was taking place. Moreover, incidence angles of 60° and 75°, whose secondary droplet plumes were more heavily subjected to scattering, did not show any ambient MS signal enhancement at longer probe distances. Interestingly, a simple calculation of the analyte fraction entering the MS, based on the area of the inlet orifice divided by the area of the desorption profile, showed a downward trend very similar to the ambient MS signal (Figure S-3). This implied that at least for incidence angles of 30° and 45°, the number of molecules entering the inlet orifice was proportional to the ambient MS signal, and that no secondary ionization processes such as desolvation due to collision with air molecules were taking place. The trend was not clear for incidence angles of 60° and 75° due to the difficulty in measuring the area of the desorption profile.

Discussion of tip height and its effect on spray impact area. The major differences between the three tip heights investigated were their effect on the enlargement of the lateral and vertical dispersions. As mentioned earlier, the spot size of the spray was expected to expand with tip height due to the diverging flow of the spray jet. Prosolia, the manufacturer of the Omni Spray ion source, observed a roughly two-fold expansion in spot size when the tip height was adjusted from 1 mm to 2 mm (Prosolia application note 117).[45] Since the spot size would depend largely on parameters such as spray flow rate, nebulizing gas pressure, and the type of substrate, ToF-SIMS was used to determine the actual spot size for the experimental conditions used in this study by imaging the distribution of the analyte on the PTFE wells before and after exposure to the DESI spray at three tip heights. As can be seen in Figure 7, the images showed the distribution of the analyte on the Teflon surface, where dark circles represented the absence of analyte. These were the locations where the spray had presumably impacted and desorbed the

analyte, which corresponded to the spot size of the spray.[31] For an incidence angle of 30°, the diameter of the spot changed from (1.3, 1.8, to 2.1) mm for tip heights of (1, 2, and 3) mm, respectively, corresponding to a factor of 2 increase for a change in tip height from 1 mm to 2 mm, and to a factor of 2.5 increase for a change in tip height from 1 mm to 3 mm. This corresponded almost exactly to the increase in observed intensity mentioned above. Therefore, at least for an incidence angle of 30°, the number of analyte removed correlated with the number of ions observed. Unfortunately, variations in spot sizes were detected only when tip height was changed. Variations in spot sizes were difficult to determine when incidence angle was changed; no differences were seen in terms of their shapes, and the edges between areas with and without analyte lacked contrast and appeared fuzzy, further complicating the assessment of the impact area.

Part of the reason why higher tip heights resulted in desorption profiles with wider dispersions was not simply due to the diverging flow of the spray, but because the entire impact area even at a tip height of 3 mm was confined within the area of the deposited sample. A great majority of the secondary droplets leaving the surface were laden with analyte. If the sample area was smaller than the spot size of the spray, the dispersion widths would probably have been smaller. A 2 μL droplet of analyte solution on the PTFE surface was found to create a circular deposit with a diameter of roughly 2.8 ± 0.2 mm. Therefore, as long as the spot size was smaller than the sample area, a majority of the secondary droplets would theoretically contain analyte and contribute to a wider dispersion length.

Although this suggested that higher tip heights with larger spot sizes would equate to more analyte desorption and hence enhanced signal, there was a problem with data reproducibility. This was because the surface concentration of the analyte differed from deposit to deposit due to the fluctuation of the deposit area (despite the deposition of an equal droplet volume). In addition, the formation of the coffee ring meant that an unknown but a large fraction of the analyte was localized around the circumference of the deposit. So unless the entire sample was consumed, DESI would have sampled an unknown fraction of the analyte deposited. To make matters worse, dimples in the PTFE surface that gave the surface its superhydrophobic character (water contact angle of 160.8 ± 2.6°) was observed to trap analyte. As can be seen in the ToF-SIMS images in Figure 7a, the coffee ring remained intact after exposure to the DESI spray. Looking closely, even some analyte inside the spray impact areas remained. The number

of analytes left behind in the spray impact area was expected to be much more than the images suggested, considering that ToF-SIMS analysis of organic molecules in the presence of chloride salts (present in methanol) and on PTFE have been seen to attenuate the analyte signal.[46] The high contact angle of the methanol/water solution (115.1 ± 2.3°) made desorption of analyte from the dimples even more difficult since the short interaction time between the impinging spray solvent and the deposited analyte would have been limited if the solvent was not wetting the surface. All of these factors implied that these barriers needed to be considered and overcome for the technique to have reduced run-to-run variability.

Conclusion

The collection experiment was able to provide important data regarding the effect of geometric configuration on the hydrodynamic properties of the DESI spray. Considering that some mass spectrometers use a vacuum suction at the inlet orifice where secondary droplets get entrained in the flow, while others have positive pressure to prevent entry of neutral species and droplets, the results presented here can be referenced to provide optimal settings for the acquisition of reproducible data for a wide variety of ambient mass spectrometry systems.

Although there are a number of parameters to consider, the ToF-SIMS data provided suggestions for how DESI should be set up to provide more reproducible results. One key finding was that reproducibility and maximum signal did not necessarily correspond with each other. While steeper incidence angles were associated with lower MS signal due to lower mass transport and material loss stemming from analyte dispersion and scattering, higher signals obtained from the use of glancing incidence angles were associated with larger error. As was shown in Figure 2, an incidence angle of 20° provided the highest signal, but was associated with a roughly 40 % run-to-run variability . It seemed that incidence angles between 25° and 35° provided the best compromise in terms of signal and reliability for this substrate and type of analyte.

For all incidence angles, shorter probe distances were found to be better since the tighter dispersion of the secondary droplet plume led to higher ion transmission into the mass spectrometer. This should be used with caution as the combination of shorter probe distances and

oblique incidence angles led to high signal variability. In comparison, longer probe distances were associated with mass loss due to the widening of the lateral and vertical dispersions.

Higher tip heights could benefit from higher ambient MS signal if the setting was combined with oblique incidence angles and shorter probe distances. Higher tip heights could potentially improve the consistency of analyte signal since the larger spot size can be used to consume the entire sample on a surface. However, there are disadvantages to using higher tip heights: larger spot sizes are not preferred for imaging applications of DESI since the spatial resolution will be degraded; and, high aspect ratio samples with large changes in surface morphology can create dramatic changes in signal intensity.

Equally important to optimizing instrument configuration was the understanding that the deposition of a sample solution onto a surface would result in a coffee ring effect, where the majority of the analyte was located on the outer circumference of the deposit. For reproducible analyses, total consumption of a sample is a requisite as well as homogeneous sample distribution on the surface. The easiest approach would be a complete consumption of the deposited sample either through the use of a larger spot size by increasing the tip height, or reducing the volume of the sample solution through precise deposition of analyte using a piezo-electric driven inkjet printer.[47]

References

1. Cotte-Rodríguez, I.; Takáts, Z.; Talaty, N.; Chen, H.; Cooks, R. G., *Analytical Chemistry* **2005,** *77* (21), 6755-6764.
2. Justes, D. R.; Talaty, N.; Cotte-Rodriguez, I.; Cooks, R. G., *Chemical Communications* **2007,** (21), 2142-2144.
3. Soparawalla, S.; Salazar, G. A.; Sokol, E.; Perry, R. H.; Cooks, R. G., *Analyst* **2010,** *135* (8), 1953-1960.
4. Takats, Z.; Cotte-Rodriguez, I.; Talaty, N.; Chen, H.; Cooks, R. G., *Chemical Communications* **2005,** (15), 1950-1952.
5. Venter, A.; Sojka, P. E.; Cooks, R. G., *Analytical Chemistry* **2006,** *78* (24), 8549-8555.
6. Dole, M.; Mack, L. L.; Hines, R. L.; Mobley, R. C.; Ferguson, L. D.; Alice, M. B., *The Journal of Chemical Physics* **1968,** *49* (5), 2240-2249.
7. Iribarne, J. V.; Thomson, B. A., *The Journal of Chemical Physics* **1976,** *64* (6), 2287-2294.
8. Takáts, Z.; Wiseman, J. M.; Cooks, R. G., *Journal of Mass Spectrometry* **2005,** *40* (10), 1261-1275.
9. Takáts, Z.; Wiseman, J. M.; Gologan, B.; Cooks, R. G., *Science* **2004,** *306* (5695), 471-473.
10. Wiseman, J. M.; Puolitaival, S. M.; Takáts, Z.; Cooks, R. G.; Caprioli, R. M., *Angewandte Chemie (English Edition)* **2005,** *117* (43), 7256-7259.
11. Eberlin, L. S.; Ifa, D. R.; Wu, C.; Cooks, R. G., *Angewandte Chemie International Edition* **2010,** *49* (5), 873-876.
12. Wiseman, J. M.; Ifa, D. R.; Song, Q.; Cooks, R. G., *Angewandte Chemie International Edition* **2006,** *45* (43), 7188-7192.
13. Kertesz, V.; Van Berkel, G. J.; Vavrek, M.; Koeplinger, K. A.; Schneider, B. B.; Covey, T. R., *Analytical Chemistry* **2008,** *80* (13), 5168-5177.
14. Chen, H.; Talaty, N. N.; Takáts, Z.; Cooks, R. G., *Analytical Chemistry* **2005,** *77* (21), 6915-6927.
15. Williams, J. P.; Scrivens, J. H., *Rapid Communications in Mass Spectrometry* **2005,** *19* (24), 3643-3650.
16. Kauppila, T. J.; Talaty, N.; Kuuranne, T.; Kotiaho, T.; Kostiainen, R.; Cooks, R. G., *Analyst* **2007,** *132* (9), 868-875.
17. Green, F. M.; Salter, T. L.; Stokes, P.; Gilmore, I. S.; O'Connor, G., *Surface and Interface Analysis* **2010,** *42* (5), 347-357.
18. Cotte-Rodríguez, I.; Mulligan, C. C.; Cooks, R. G., *Analytical Chemistry* **2007,** *79* (18), 7069-7077.
19. Ifa, D. R.; Gumaelius, L. M.; Eberlin, L. S.; Manicke, N. E.; Cooks, R. G., *Analyst* **2007,** *132* (5), 461-467.
20. Fernandez, F. M.; Hostetler, D.; Powell, K.; Kaur, H.; Green, M. D.; Mildenhall, D. C.; Newton, P. N., *Analyst* **2011,** *136* (15), 3073-3082.
21. Talaty, N.; Mulligan, C. C.; Justes, D. R.; Jackson, A. U.; Noll, R. J.; Cooks, R. G., *Analyst* **2008,** *133* (11), 1532-1540.
22. Weston, D. J., *Analyst* **2010,** *135* (4), 661-668.
23. Green, F. M.; Stokes, P.; Hopley, C.; Seah, M. P.; Gilmore, I. S.; O'Connor, G., *Analytical Chemistry* **2009,** *81* (6), 2286-2293.
24. Hu, Q.; Talaty, N.; Noll, R. J.; Cooks, R. G., *Rapid Communications in Mass Spectrometry* **2006,** *20* (22), 3403-3408.
25. Kaur-Atwal, G.; Weston, D. J.; Green, P. S.; Crosland, S.; Bonner, P. L. R.; Creaser, C. S., *Rapid Communications in Mass Spectrometry* **2007,** *21* (7), 1131-1138.
26. Douglass, K.; Jain, S.; Brandt, W.; Venter, A., *Journal of The American Society for Mass Spectrometry* **2012,** *23* (11), 1896-1902.
27. Gurdak, E.; Salter, T.; Smith, S.; Seah, M.; Gilmore, I.; Green, F., **2013**.
28. Volny, M.; Venter, A.; Smith, S. A.; Pazzi, M.; Cooks, R. G., *Analyst* **2008,** *133* (4), 525-531.

29. Forbes, T. P.; Brewer, T. M.; Gillen, G., *Applied Physics Letters* **2013,** *102* (21), 214102-4.
30. Kertesz, V.; Van Berkel, G. J., *Rapid Communications in Mass Spectrometry* **2008,** *22* (17), 2639-2644.
31. Pasilis, S. P.; Kertesz, V.; Van Berkel, G. J., *Analytical Chemistry* **2007,** *79* (15), 5956-5962.
32. Wiseman, J. M.; Ifa, D. R.; Venter, A.; Cooks, R. G., *Nat. Protocols* **2008,** *3* (3), 517-524.
33. Costa, A. B.; Cooks, R. G., *Chemical Communications* **2007,** (38), 3915-3917.
34. Costa, A. B.; Graham Cooks, R., *Chemical Physics Letters* **2008,** *464* (1–3), 1-8.
35. Szakal, C.; Brewer, T. M., *Analytical Chemistry* **2009,** *81* (13), 5257-5266.
36. Gillen, G.; Szakal, C.; Brewer, T. M., *Surface and Interface Analysis* **2011,** *43* (1-2), 376-379.
37. Covey, T. R.; Thomson, B. A.; Schneider, B. B., *Mass Spectrometry Reviews* **2009,** *28* (6), 870-897.
38. Cech, N. B.; Enke, C. G., *Mass Spectrometry Reviews* **2001,** *20* (6), 362-387.
39. Hardware Manual: API 4000 LC/MS/MS System. http://www.absciex.com/Documents/Downloads/Literature/4000-api-hardware-guide.pdf.
40. Ifa, D. R.; Manicke, N. E.; Rusine, A. L.; Cooks, R. G., *Rapid Communications in Mass Spectrometry* **2008,** *22* (4), 503-510.
41. Marple, V. A.; Liu, B. Y. H., *Environmental Science & Technology* **1974,** *8* (7), 648-654.
42. Burwash, W.; Finlay, W.; Matida, E., *Aerosol Science and Technology* **2006,** *40* (3), 147-156.
43. Oh, J.-S.; Olabanji, O. T.; Hale, C.; Mariani, R.; Kontis, K.; Bradley, J. W., *Journal of Physics D: Applied Physics* **2011,** *44* (15), 155206.
44. Muramoto, S.; Forbes, T. P.; Staymates, M. E.; Gillen, G., *Analyst* **2014,** *139* (11), 2668-2673.
45. The Effect of Nebulizing Gas Pressure, Volumetric Flow Rate and Tip-to-Surface Distance on Spot Size in DESI-MS. http://www.prosolia.com/resources/application-notes.
46. Wagner, M. S.; McArthur, S. L.; Shen, M.; Horbett, T. A.; Castner, D. G., *Journal of Biomaterials Science, Polymer Edition* **2002,** *13* (4), 407-428.
47. Verkouteren, R. M.; Verkouteren, J. R., *Analytical Chemistry* **2009,** *81* (20), 8577-8584.

Figure Captions

Figure 1. (a) Schematic representation of the DESI source showing the instrument parameters that were investigated for this study; incidence angle, tip height, and probe distance. (b) Schematic showing the collector with a manual shutter that limited the exposure time of the secondary droplets, and the position of the MS inlet with respect to the sample surface (note that the inner diameter of the inlet sits flush with the sample surface). Since the center of the PTFE deposition areas closest to the edge was 3 mm from the end of the slide, the minimum probe distance was 3 mm. (c) ToF-SIMS image of the Si collector (14 mm × 10 mm image), showing the desorption profile (spatial distribution) of the analyte post-exposure to the DESI spray. The width and height of the profile were referred to as the lateral and vertical dispersions, respectively.

Figure 2. (a) ToF-SIMS ion images of the collectors showing the change in the desorption profile (spatial distribution) of analyte as a function of incidence angle (14 mm × 7 mm image size), captured at a probe distance of 3 mm and a tip height of 1 mm. The collector was exposed to the DESI spray for 10 s. The blue circle with the gray halo seen in the 20° image represents the dimensions of the ambient MS inlet, where the blue is the 1 mm ID inlet orifice, and grey is the 3 mm OD cylinder. The size of the drawing is the actual size in relation to the desorption profile images. (b) ToF-SIMS intensity of cocaine at *m/z* 304 on the collectors (normalized to Si^+ at *m/z* 28) as a function of incidence angle. (c) Ambient MS intensity for the same incidence angles, acquired over (1, 3, and 5) min durations.

Figure 3. ToF-SIMS ion images of the collectors showing the change in the desorption profile of analyte as a function of probe distance at incidence angles of (a) 30°, (b) 45°, (c) 60°, and (d) 75°. Probe distances of (3, 5, 7, 9, and 11) mm were investigated for tip heights of (1, 2, and 3) mm. Image size is 14 mm × 7 mm. The collectors were exposed to the DESI spray for 10 s.

Figure 4. Lateral and vertical dispersions of the desorption profiles plotted as a function of probe distance at incidence angles of 30°, 45°, 60°, and 75° and at tip heights of (1, 2, and 3) mm. The solid and open markers represent data points for lateral and vertical dispersions, respectively. Lines fits were presented only for lateral dispersions to facilitate viewing.

Figure 5. Lateral and vertical dispersion angles of the desorption profiles plotted as a function of probe distance at incidence angles of 30°, 45°, 60°, and 75° and at tip heights of 1 mm, 2 mm, and 3 mm. The solid and open markers represent data points for lateral and vertical dispersion angles, respectively. Lines fits were presented only for lateral dispersion angles to facilitate viewing. The angles were calculated using the dispersion lengths presented in Figure 4. The values presented are overestimates since the angles were calculated assuming that the origin of the dispersion (impact point of the DESI spray) was a point, and not the actual spot size.

Figure 6. QTrap (ambient MS) intensities of the analyte plotted as a function of probe distance at incidence angles of 30°, 45°, 60°, and 75° and at tip heights of (1, 2, and 3) mm. The height of

the inlet tube relative to the sample surface was adjusted by up to 0.5 mm to accommodate a wider vertical distribution of the secondary droplets for longer probe distances. Each data point represents an average of three runs. For each run, the signal was acquired over 3 min. Probe distance here refers to the distance between the DESI impact point and the tip of the MS inlet capillary. 200 ng of analyte was sampled for each run.

Figure 7. (a) ToF-SIMS images of the cocaine molecule distributed on the Teflon surface, before exposure to DESI at 30° incidence angle (control), and after 10 s exposure at tip heights of 1 mm, 2 mm, and 3 mm. The circles with the dotted lines marked the areas where analyte appeared to be absent. Lighter color indicates higher intensity. The direction of the DESI spray was from left to right. 2μL aliquots of 100 μg/mL solution of cocaine were deposited at each well. (b) Optical micrograph of the 3.5 mm diameter Teflon surface of the Omni Slide, showing the 100 μm diameter dimples with an rms roughness of approximately 9.1 ± 2.1 μm. Contact angles on the Teflon surface for (c) MeOH/H_2O solution was 115.1 ± 2.3°, and for (d) pure water was 160.8 ± 2.6°.

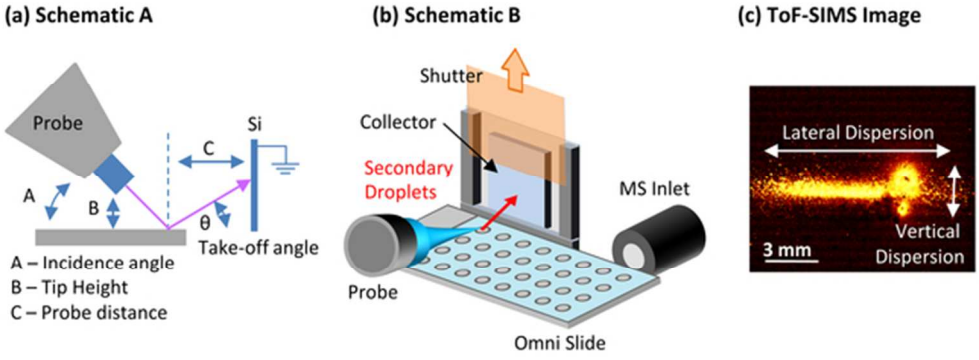

55x20mm (300 x 300 DPI)

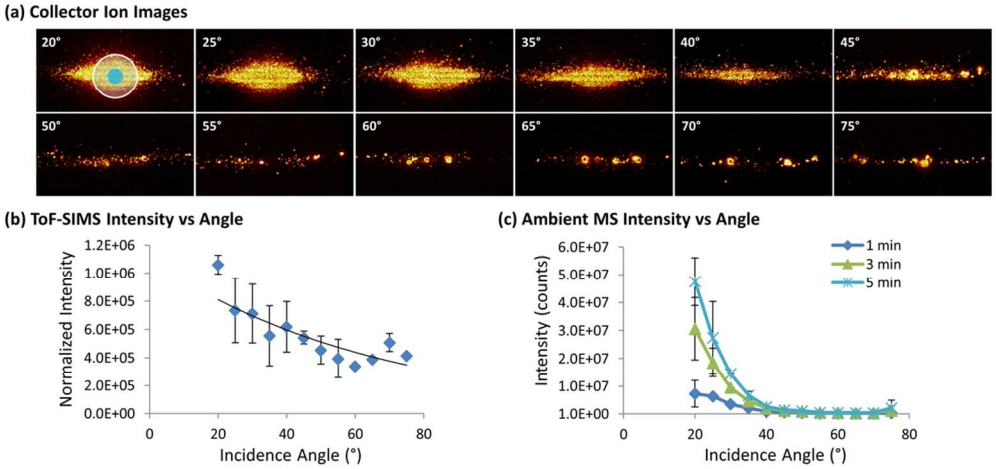

106x50mm (300 x 300 DPI)

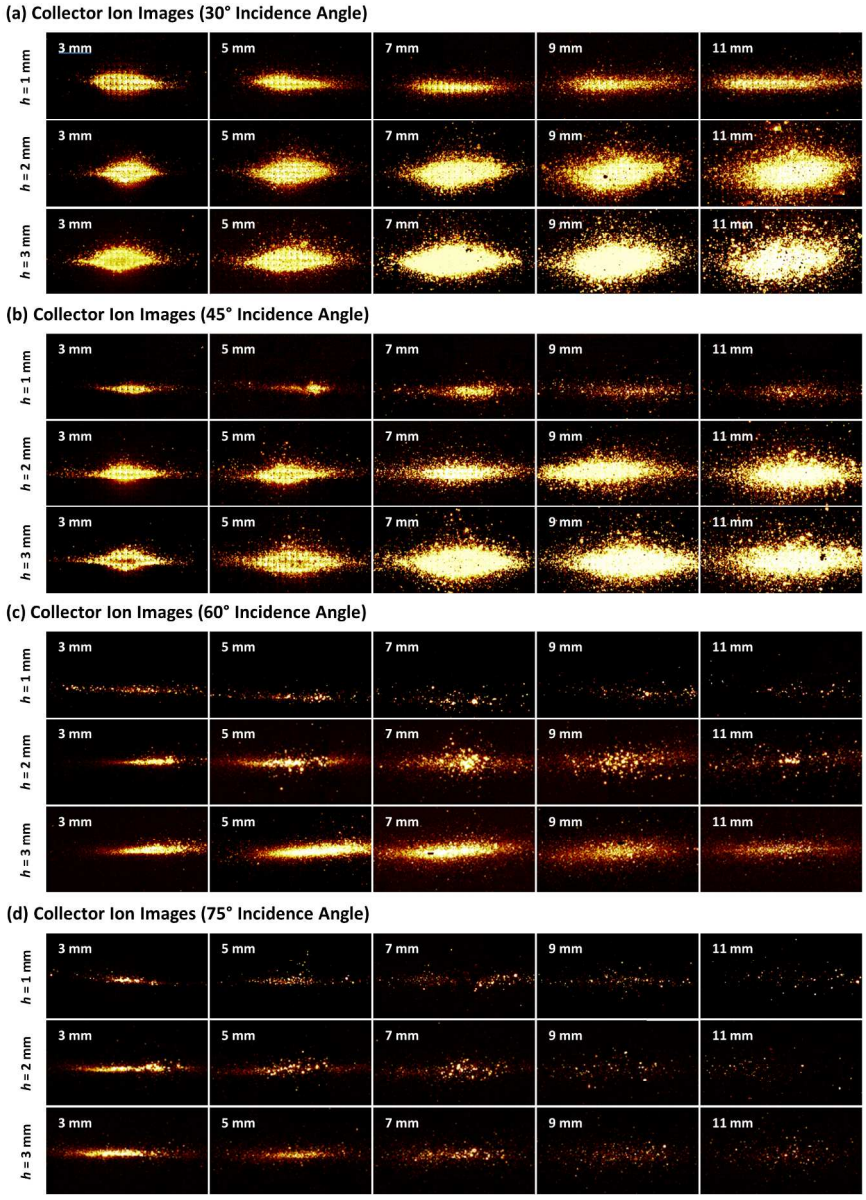

190x264mm (295 x 295 DPI)

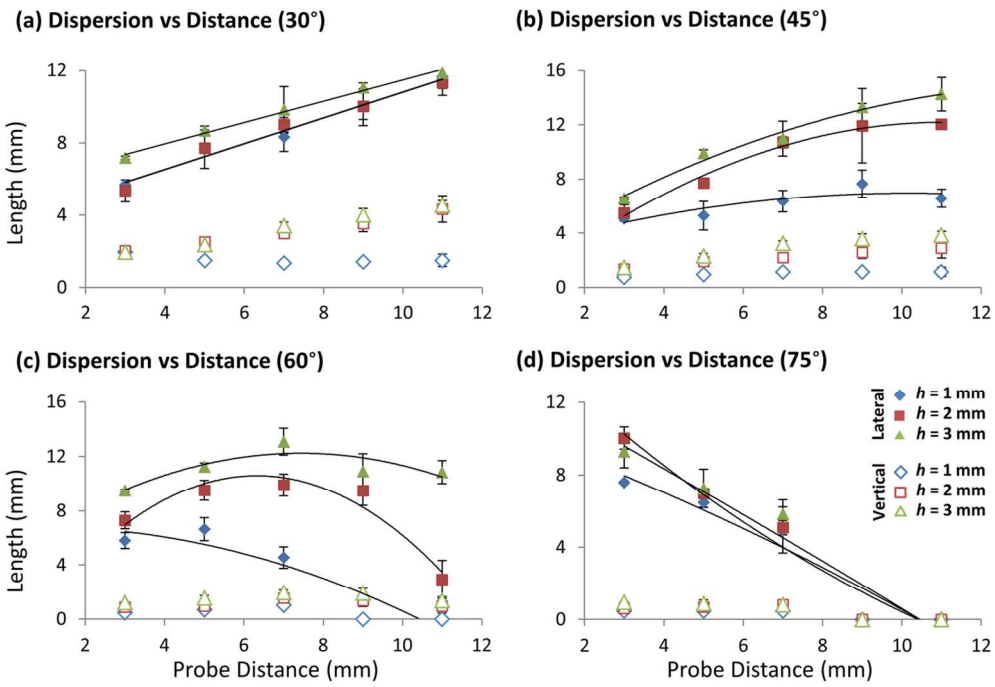

119x81mm (300 x 300 DPI)

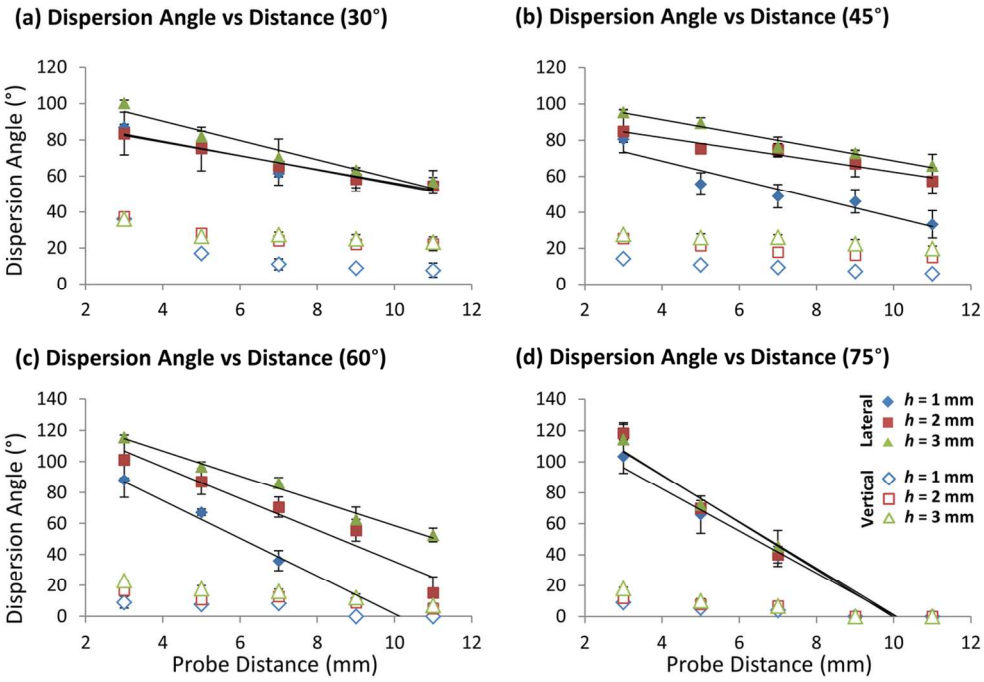

119x81mm (300 x 300 DPI)

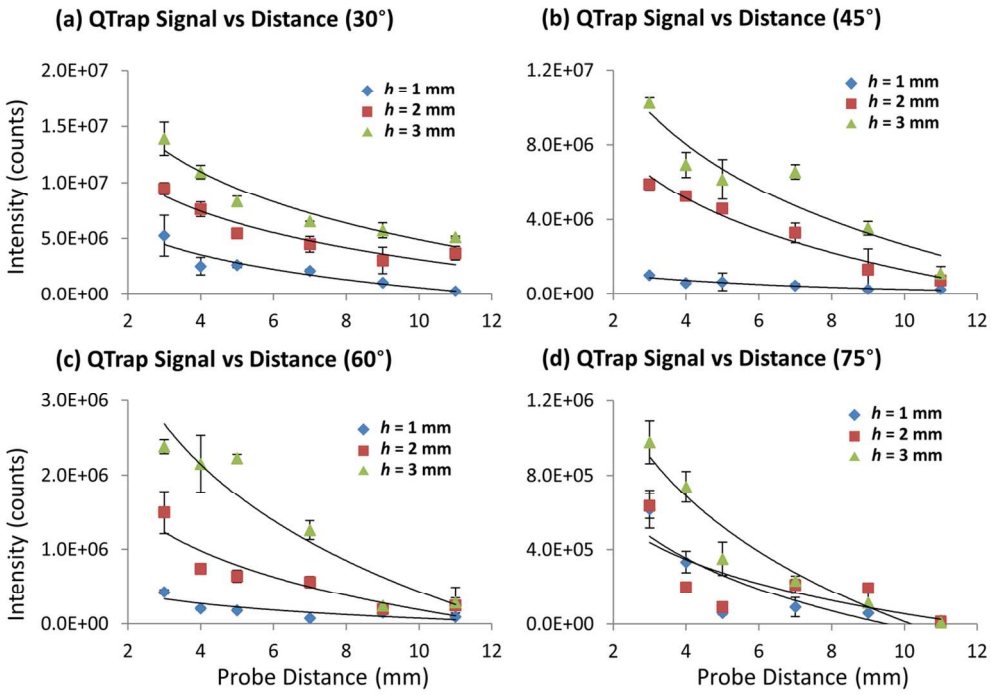

119x83mm (300 x 300 DPI)

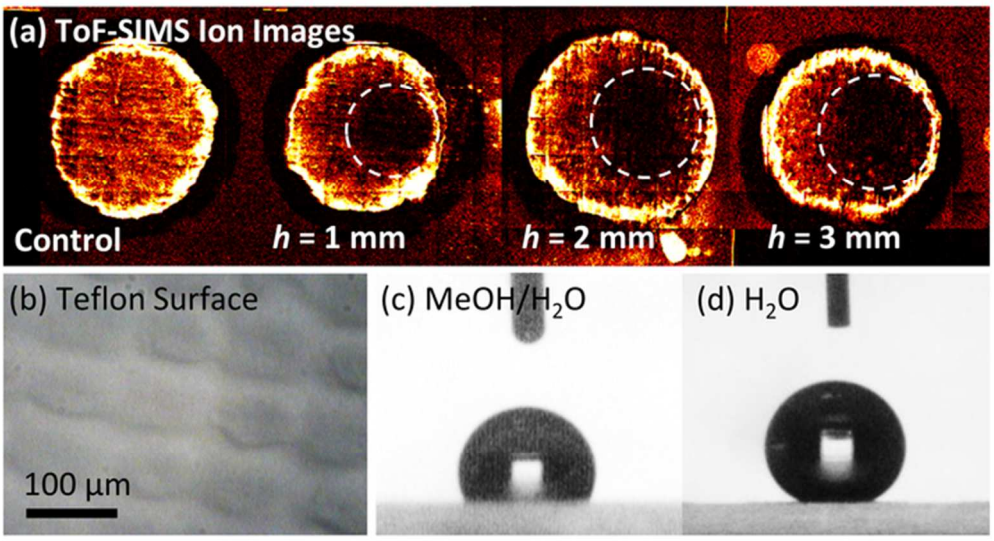

60x33mm (300 x 300 DPI)